2D Materials

PAPER

Two-dimensional $PdSe_2$-Pd_2Se_3 junctions can serve as nanowires

To cite this article: Sebastian Zuluaga *et al* 2018 *2D Mater.* **5** 035025

Two-dimensional $PdSe_2$-Pd_2Se_3 junctions can serve as nanowires

Sebastian Zuluaga[1], Junhao Lin[2], Kazu Suenaga[2,3], Sokrates T. Pantelides[1,4]

[1]Department of Physics and Astronomy, Vanderbilt University, Nashville, TN, USA
[2]National Institute of Advanced Industrial Science and Technology (AIST), AIST Central 5, Tsukuba 305-8565, Japan
[3]Department of Mechanical Engineering, The University of Tokyo, Tokyo 113-8656, Japan
[4]Department of Electrical Engineering and Computer Science, Vanderbilt University, Nashville, TN, USA

Abstract. While the exfoliation of almost all layered materials results in a monolayer with the same atomic geometry as its bulk counterpart, the exfoliation of $PdSe_2$ results in a monolayer with a different atomic geometry and a new stoichiometry, Pd_2Se_3, which is a fusion of two $PdSe_2$ monolayers mediated by Se emission. Here we first report first-principles calculations of lateral junctions between a $PdSe_2$ bilayer and a Pd_2Se_3 monolayer. We find that, while several distinct junction geometries are possible, they all exhibit empty interface states below the conduction band. As a result, light n-type doping of either or both sides, e.g., by halogen atoms replacing Se atoms, leads to a remotely-doped interface, i.e., a one-dimensional conducting nanowire that runs along the junction, in between the two semiconductors. We have fabricated such junctions inside a scanning transmission electron microscope (STEM), but doping and transport measurements are not currently practical.

Keywords: Lateral Junction, $PdSe_2$ bilayer, Pd_2Se_3 monolayer, empty interface states, conducting nano wire.

1. Introduction

In layered materials, the weak van der Waals interactions between layers allow the exfoliation of monolayers. As a result, monolayers typically have the same atomic geometry as their counterparts in the bulk material. The best example of such materials is graphene, which has attracted extensive attention. However, the absence of a band gap makes graphene unsuitable for nano-electronics and other applications. As a result, the search, discovery, and fabrication of new two-dimensional (2D) materials has been a major research focus. For example, transition-metal dichalcogenides have attracted significant attention [1–3] due to potential applications in the fields of electronics [4], optoelectronics [5], and other areas [6–9]. Recently, atomically-sharp lateral junctions between 2D transition-metal dichalcogenides have been fabricated, creating heterostructures that exhibit localized photoluminescence enhancement and form p-n diodes and photodiodes [10–14].

$PdSe_2$ is a layered system that has been investigated in part because its electronic properties depend on the number of layers [15–18] and because of its catalytic activity [19, 20]. Density-functional-theory (DFT) calculations have shown that the value of the band-gap ranges from 0.03 eV to 1.43 eV as the system goes from the bulk to a monolayer [17]. However, experimentalists have found it difficult to fabricate free-standing $PdSe_2$ monolayers. Recently, Oyedele et.al [18] reported experimental data on exfoliated $PdSe_2$ monolayers, but atomic-resolution Z-contrast images show good agreement only with the expected atomic positions, while the intensities deviate significantly from simulated intensities. The differences were attributed to either defects or instabilities that may arise in a free-standing monolayer but not necessarily in monolayers on a substrate such as SiO_2. At about the same time, on the other hand, we reported that attempts to exfoliate a $PdSe_2$ monolayer resulted in a Pd_2Se_3 monolayer, which was demonstrated to arise from the fusion of two $PdSe_2$ monolayer, mediated by the emission of Se atoms [21]. The same result was obtained when the bulk material was thinned using the electron beam of a scanning transmission electron microscope. The band gap of the monolayer Pd_2Se_3 was calculated to be 1.12 eV [21]. Due to the novelty, further properties of this 2D material have not been studied so far.

In the present work, we begin by using DFT calculations to explore the possibility of constructing lateral junctions between a $PdSe_2$ bilayer and a Pd_2Se_3 monolayer. We found that there are several distinct bonding possibilities, but in all cases, once the $PdSe_2$-Pd_2Se_3 junction is formed, empty interface states appear just below the conduction band. Effectively, the junction forms a one-dimensional channel where the band-gap is smaller than in other parts away of the junction. The results lead us to predict that if we dope the sample n-type using Cl, Br or any other atom that donates one electron to the system, we will obtain a one-dimensional conducting nanowire running along the junction. We have fabricated such junctions and characterized them using atomic-resolution scanning-transmission-electron-microscope (STEM) images. However, the doping and fabrication of contacts for transport measurements of the one-dimensional conducting nanowire are not practical at this point and are left for future work.

2. Computational details

Density functional theory calculations (DFT) were performed using the VASP code [22–24], with projector-augmented-wave (PAW) pseudopotentials [25] and a plane-wave expansion with a kinetic energy cutoff of 500 eV. In order to simulate the $PdSe_2$-Pd_2Se_3 junction we constructed a system with dimensions 68.88 Å $\times$ 5.89 Å$\times$ 18.00 Å (12 times longer in the x direction than the regular

unit cell of $PdSe_2$), where in one half of the super cell we have the $PdSe_2$ bilayer and on the other half we have the Pd_2Se_3 monolayer, with the junctions at the middle and at the boundary of the supercell.

Due to the dimensions of the unit cell, we used a 1×5×1 grid for the **k**-point sampling centered around the Γ point. All atoms were relaxed until the forces were smaller that 0.001 eV/Å. The density of states was obtained by performing hybrid functional calculations using the HSE06 functional as implemented in VASP.

The lattice optimization calculations show that while the $PdSe_2$ bilayer exhibits an in-plane lattice constant of 5.74×5.89 Å, the Pd_2Se_3 monolayer exhibits an in-plane lattice constant of 5.93×6.02 Å. Since we will be working with a $PdSe_2$-Pd_2Se_3 junction, and the Pd_2Se_3 monolayer is created by the exfoliation of small $PdSe_2$ bilayer patches, we use the lattice constants of the $PdSe_2$ bilayer through all the systems in this work. The van der Waals interactions were taken into account using the D2 method of Grimme (DFT-D2) [26].

3. Experimental details

The bulk $PdSe_2$ sample was synthesized by chemical vapor transport (CVT) method. The few-layer sample was prepared by mechanical exfoliation onto a SiO_2/Si substrate, which was subsequently moved to a Au quantifoil TEM grid by a dry-transfer method. Z-contrast STEM imaging was done in a JEOL 2100F with delta probe corrector, which corrects the aberration up to 5th order, resulting in a probe size of 1.4 Å. The imaging was conducted at an acceleration voltage of 60 kV. The convergent angle for illumination was about 35 mrad, with a collection detector angle ranging from 62 to 200 mrad. A JEOL heating-holder was used to gently warm up the sample to 160 °C to evaporate any residual chemicals on the surface of the sample, which can effectively reduce carbon re-deposition during the examination of the sample. For more information concerning the exfoliation of the $PdSe_2$, and the synthesis of the Pd_2Se_3 monolayer please see Ref. [21].

4. Results-DFT

Theoretically, the $PdSe_2$-Pd_2Se_3 junction can take place in 64 different ways, both of the $PdSe_2$ layers and the Pd_2Se_3 layer have four possible terminations (Please see the Supplementary Material for more details on how the junctions are constructed). After examining many possible configurations, we found that the junctions can be divided in two main groups; in the first group the junction takes place mainly trough the bonding of one of the layers in the $PdSe_2$ bilayer with the Pd_2Se_3 monolayer, while in the second group both layers of the PdS_2 system equally engage in the bonding with the Pd_2Se_3 monolayer. In this work, we have chosen one example of each group and will refer to these two junction configurations as α and β. In Figure 1 we show top and a side views of the two junctions. The calculations show that the binding energies between the bilayer and the monolayer, namely the energies required to pull the bilayer and monolayer infinitely apart, only differ in 0.61 eV between the α and β junctions, this small difference between the two of them tells us that there is not a strong energetic preference of one configuration over the other.

The total and projected densities of states (TDOS and PDOS) of the α and β junctions are shown in Figure 2. The PDOS on atoms far from the interface, (lower four panels) reveal that, as expected, the two materials retain the energy gaps of the corresponding pristine materials, namely 1.43 eV for $PdSe_2$ and 1.12 eV for Pd_2Se_3. We note that the agreement with the energy

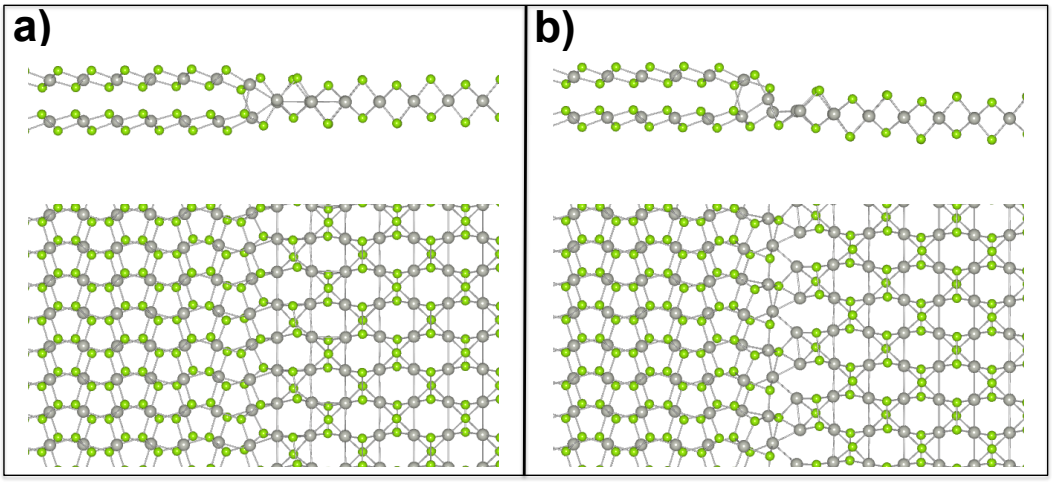

Figure 1. $PdSe_2$-Pd_2Se_3 junctions. Panels a) and b) show the junctions labeled as α and β, respectively. In each panel the upper figures show the side view of the system, while the lower figures show the top view of the junction. Grey and green spheres denote Pd and Se atoms, respectively.

gaps of the pristine materials is only approximate because, even though the Pd and Se atoms that are used to calculate the PDOS are located ∼14 Å away from the junction, small effects of the junctions propagate down to these Pd and Se atoms altering their electronic structure. For the same reason, the PDOS on Pd and Se atoms far from the interface in the α junction do not match exactly the PDOS on corresponding atoms in the β junction. On the other hand, the PDOS on atoms in the vicinity of the interface demonstrate that the states within the energy gap are fairly localized in the interfacial region, i.e., they correspond to empty interface states.

The localization of the empty interface states can be visualized by plotting the square of the wave functions corresponding to the states that are localized at the interface in the middle of the band gap. As an example, in Figure 3 we have plotted the square of the wave function corresponding to the states localized around 0.5 eV of Figure 2 for the β junction.

The results presented in Figures 2 and 3 reveal that the $PdSe_2$-Pd_2Se_3 junction has unoccupied interface states, namely states that are localized in a narrow interfacial stripe, within the common energy gap as illustrated in Figure 4a. Such electronic structure resembles what is known to occur in quantum wells, e.g., formed in a $Al_xGa_{1x}As$ – GaAs – $Al_xGa_{1x}As$ heterostructure [27], which is shown schematically in Figure 4b. It has long been established that, if the $Al_xGa_{1x}As$ regions are doped n-type, dopant electrons naturally leave the conduction bands of these regions and occupy the lower-energy states that are localized in the GaAs quantum well. The bands bend by electrostatic potentials arising from the charge separation. The process is known as modulation doping and is the principle that underlies the fabrication of high-electron mobility transistors (HEMTs) [28]. The high mobility arises because the ionized impurities are not in the conducting channel and Coulomb scattering is minimized. In the present case, if the $PdSe_2$ bilayer and Pd_2Se_3 monolayer are doped n-type, the dopant electrons from these layers would again leave the conduction bands and occupy the lower-energy interface states where they form a one-dimensional electron gas (1DEG). The net result is a one-dimensional conductor with high mobility because of the separation of the ionized donors from the conducting carriers at the interface. The band diagram is as shown in Figure 4c.

Table 1 shows the energy required to replace one Se atom with Br or Cl in the $PdSe_2$ bilayer and Pd_2Se_3 monolayer. $PdSe_2$ bilayers have only one type of Se atoms while the Pd_2Se_3 monolayers

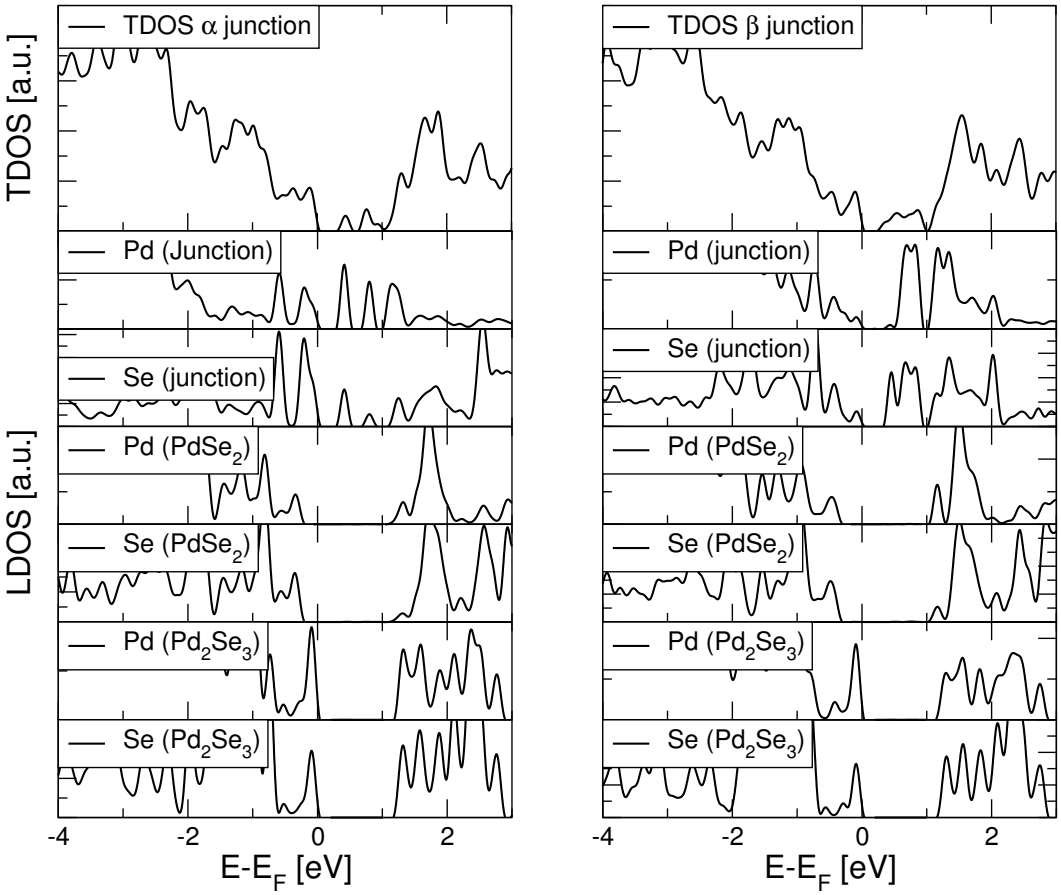

Figure 2. Density of states of junctions α and β are shown in the left and right hand side panels, respectively. While the upper part of the figure shows the TDOS, the lower panels show the PDOS on Pd and Se atoms located at the junction, the middle of the $PdSe_2$ section, and the middle of Pd_2Se_3 section.

have two non-equivalent Se atoms (one binds to two Pd atoms, while the second binds to four Pd atoms). In Table 1, configurations 1 and 2 denote the cases where the Se atom being replaced is the one bonded to two and four Pd atoms, respectively. The negative values in the table denote that the replacement is energetically favorable (exothermic process), while a positive value denotes the energy needed to dope the material (endothermic process). The table shows that in most cases the doping is energetically favorable, and in the cases that it is not, the energy required for the doping is small (less than 0.1 eV). Due to the number of atoms in the system, and the low concentration of Cl or Br atoms needed to dope the material without drastically changing the electronic structure, it is not possible to perform a DFT calculation for such a doped system.

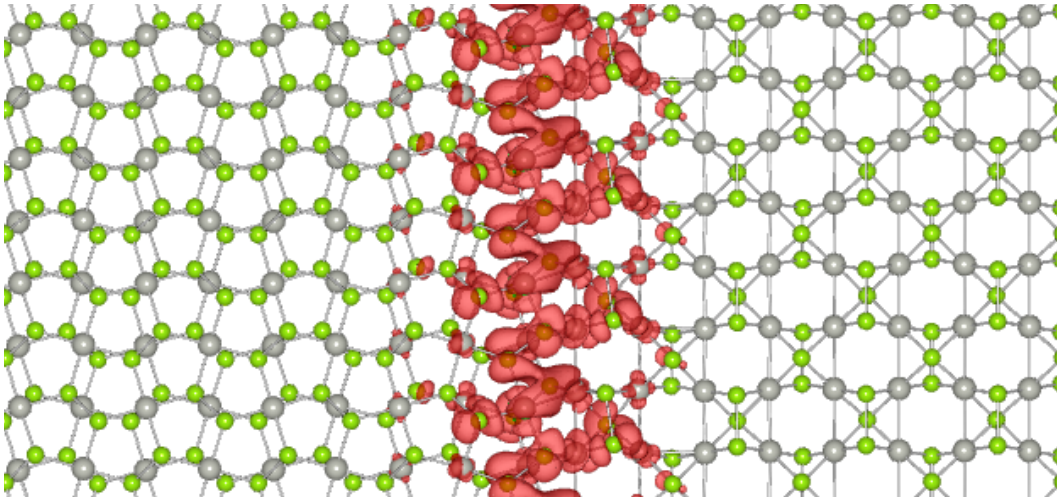

Figure 3. Square of the wave function of the empty interface states (localized around 0.5 eV in Figure 2) in the β junction. The square of the wave function is shown as red globes around the atoms. The iso surface was set to 6×10^{-4} $e/\text{Å}^3$. Grey and green spheres denote Pd and Se atoms, respectively.

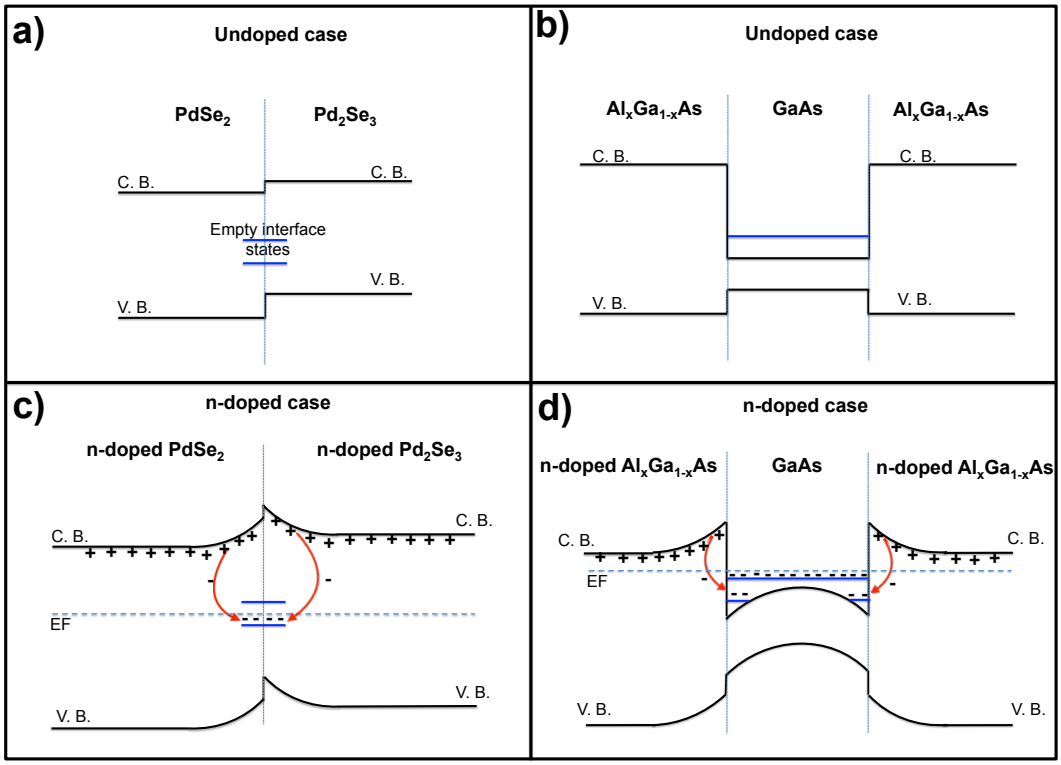

Figure 4. Schematic comparison of the bands at the bilayer-monolayer junction before and after n-doping for the $PdSe_2$-Pd_2Se_3 (a,c) and a $Al_xGa_{1x}As$–GaAs–$Al_xGa_{1x}As$ quantum well (b,d). The lower panels of the figure show that electrons from the ionized donors indicated by the + signs occupy lower-energy states that are localized at the junction (c) or quantum well (d). (the "+" and "-" signs indicate ionized donors and electrons, respectively;). VB and CB label the valence and conduction band edges, respectively.

In order to determine the valence-band offsets at the $PdSe_2$-Pd_2Se_3 junction, we have calculated the average potential in planes perpendicular to the α junction and plotted them as a function of the distance along the x axis, as shown in Figure 5. The figure shows a 0.39 eV

Table 1. Energy required to dope the $PdSe_2$ bilayer and the Pd_2Se_3 monolayer with Cl and Br atoms. We assume that the source of Cl and Br atoms are Cl_2 and Br_2 molecules and that the replaced Se atoms goes into Se bulk after leaving the $PdSe_2$ bilayer or the Pd_2Se_3 monolayer. All energies are in eV.

System	Cl	Br
$PdSe_2$	-0.02	0.04
Pd_2Se_3 config. 1	-0.32	-0.23
Pd_2Se_3 config. 2	0.09	0.06

difference in the average potential between the $PdSe_2$ and Pd_2Se_3 region. On the other hand, we have calculated tha the valence band maxima of the $PdSe_2$ bilayer and Pd_2Se_3 monolayer are located 0.97 and 0.94 eV below the average potentials of the $PdSe_2$ bilayer and Pd_2Se_3 monolayer, respectively. Therefore, we can conclude that the $PdSe_2$-Pd_2Se_3 junction is a staggered-gap (type II) junction, where the valence band maxima (VBM) of the $PdSe_2$ bilayer is located 0.42 eV below the valence band maxima of the Pd_2Se_3 monolayer (see Figure 5). It is important to mention that it is not possible to align the bands using only the information provided in Figure 2 because the Pd and Se atoms, in the $PdSe_2$ and Pd_2Se_3 regions, are too close to the junction and feel the effects of band bending.

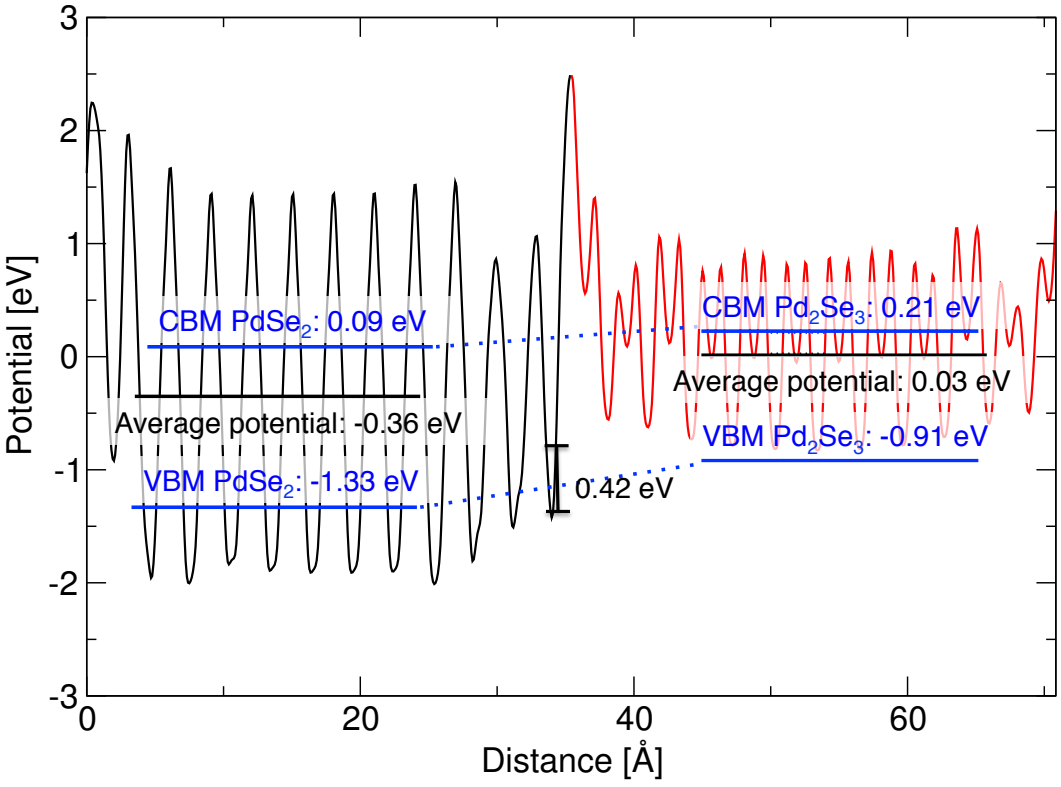

Figure 5. Average potential of perpendicular planes across the α junction. The $PdSe_2$ region is plotted in black, while the Pd_2Se_3 region is plotted in red. The Figure indicates the averga potential of each region, as well as the relative position of the valence band maxima (VBM) and the conduction band minima (CBM) in both regions.

5. Results-experiment

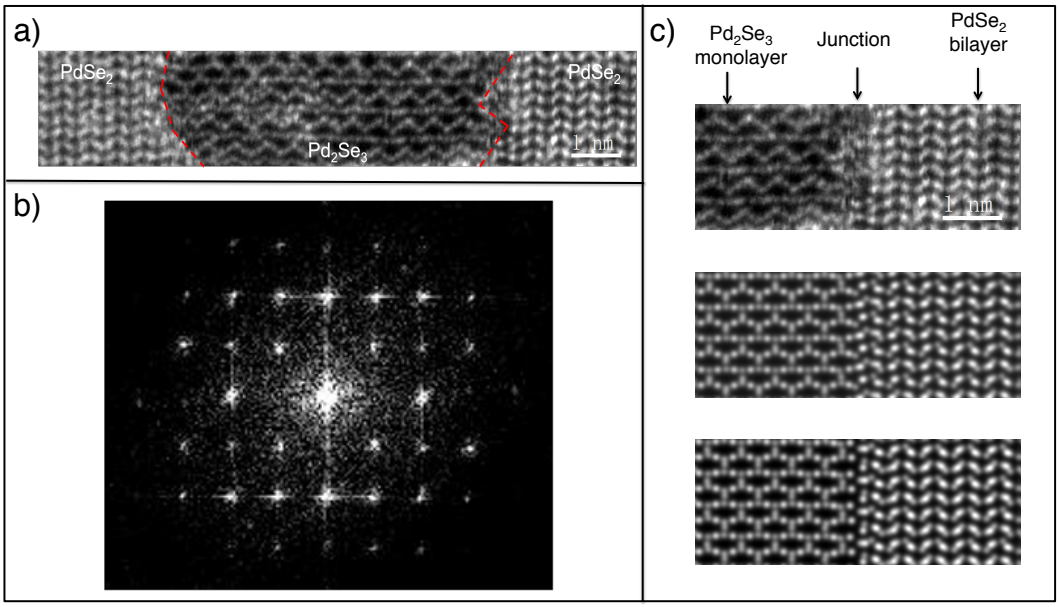

Figure 6. Panel a): Large area STEM image showing two interfaces between the $PdSe_2$ bilayer and the Pd_2Se_3 monolayer. The interface regions are highlighted by red dashed lines. Panel b): fast Fourier transform of the region shown in panel a). Pane c): the upper panel shows the STEM image of the junction between the $PdSe_2$ bilayer and the Pd_2Se_3 monolayer. The Lower panels show the STEM image simulation based on the α and the β. Details for the experimental STEM images and the simulated images are provided in SI.

A pair of monolayer-bilayer junctions were fabricated using the electron beam to induce interlayer fusion in a $PdSe_2$ bilayer region of a $PdSe_2$ sample as described in prior work [21]. The Pd_2Se_3 monolayer is formed by the emission of Se atoms from the bilayer, induced by electron irradiation. An atomic-resolution STEM image of the pair of junctions is shown in Figure 6a. The interface regions are highlighted by red dashed lines, displaying an irregular shape including sharp turning angles. Nevertheless, the fast Fourier pattern of this area, shown in Figure 6b shows only one set of square diffraction patterns, which suggests the $PdSe_2$ bilayer and Pd_2Se_3 monolayer share the same orientation while forming a junction without a well-defined shape of the interface.

In Figure 6c, we display again the STEM image of one of the two $PdSe_2$-Pd_2Se_3 junctions (upper panel) and simulated STEM images based on the α and β theoretical junctions (lower panels). While there is a strong resemblance between the two figures, the experimental STEM (upper panel) shows that the junction is not sharp, which suggests that the junction does not necessarily comprise a single configuration. It is likely that the slight disorder that is visible at the experimental interface maybe caused by an admixture of more than one bonding configurations. This possibility is consistent with the results presented earlier where we show that the binding energies of two different junction configurations are similar (less than 0.11 eV/Å apart), which indicates that there is no strong preference of one configuration over the other. Moreover, different configurations show similar properties of the interface (see Supplementary Material), suggesting the experimentally achievable interface with mixed configurations also leads to a 1D conductive channel within the 2D sheet.

6. Conclusions

In this work we investigate lateral junctions between $PdSe_2$ bilayers and Pd_2Se_3 monolayers. The results indicate that while a junction can form 64 different configurations or atomic geometries, all of the investigated interfaces resulted in the creation of empty interface states in the system's band gap. The results show that these states are localized only at the Pd and Se atoms participating in the junction. Other atoms away from the junction exhibit the PDOS corresponding to the PDOS found in the pristine $PdSe_2$ bilayer and the Pd_2Se_3 monolayer.

Based on our results, we predict that if we dope the junction with Cl or Br atoms, we should obtain a one dimensional conducting nanowire, running along the junction. The calculations indicate that in most cases, depending on the Se atoms being replaced and the atom replacing it (Cl or Br), the doping is exothermic. In the cases where the process is endothermic, the required energy for the doping is small, up to 0.1 eV. We report fabrication of junctions between $PdSe_2$ bilayers and Pd_2Se_3 monolayers and characterization by atomic-resolution STEM images. While at the moment the doping and measurement of the one-dimensional conducting nanowire are not possible, we expect that the present work will trigger future work for such investigations.

Acknowledgments

Theoretical work at Vanderbilt (S. Z. and S. T. P.) was supported in part by Department of Energy grant DE-FG02-09ER46554 and by the McMinn Endowment. The experimental work at AIST, Tsukuba, was supported by the Japan Science and Technology Agency (JST)-ACCEL and the Japan Society for the Promotion of Science (JSPS) KAKENHI (Grants No. JP16H06333 and No. P16823).

7. References

[1] Yun W S, Han S W, Hong S C, Kim I G and Lee J D 2012 *Phys. Rev. B* **85**(3) 033305
[2] Xu X, Yao W, Xiao D and Heinz T F 2014 *Nat. Phys.* **10** 343–350
[3] Komsa H P, Kotakoski J, Kurasch S, Lehtinen O, Kaiser U and Krasheninnikov A V 2012 *Phys. Rev. Lett.* **109**(3) 035503
[4] Jariwala D, Sangwan V K, Lauhon L J, Marks T J and Hersam M C 2014 *ACS Nano* **8** 1102–1120 (*Preprint* `http://dx.doi.org/10.1021/nn500064s`)
[5] Wang Q H, Kalantar-Zadeh K, Kis A, Coleman J N and Strano M S 2012 *Nat. Nanotechnol.* **7** 699–712
[6] Xia J, Yan J and Shen Z X 2017 *FlatChem* **4** 1 – 19
[7] Molas M R, Faugeras C, Slobodeniuk A O, Nogajewski K, Bartos M, Basko D M and Potemski M 2017 *2D Materials* **4** 021003
[8] Wang Z, Zhao L, Mak K F and Shan J 2017 *Nano Lett.* **17** 740–746
[9] Li Z and Wong S L 2017 *Mater. Sci. Eng. C.* **70** 1095–1106 recent Advances in Biomedical Materials
[10] Gong Y, Lin J, Wang X, Shi G, Lei S, Lin Z, Zou X, Ye G, Vajtai R, Yakobson B I, Terrones H, Terrones M, Tay B K, Lou J, Pantelides S T, Liu Z, Zhou W and Ajayan P M 2014 *Nat. Mater.* **13** 1135–1142
[11] Li M Y, Shi Y, Cheng C C, Lu L S, Lin Y C, Tang H L, Tsai M L, Chu C W, Wei K H, He J H, Chang W H, Suenaga K and Li L J 2015 *Science* **349** 524–528
[12] Duan X, Wang C, Shaw J C, Cheng R, Chen Y, Li H, Wu X, Tang Y, Zhang Q, Pan A, Jiang J, Yu R, Huang Y and Duan X 2014 *Nat. Nanotechnol.* **9** 1024–1030
[13] Huang C, Wu S, Sanchez A M, Peters J J P, Beanland R, Ross J S, Rivera P, Yao W, Cobden D H and Xu X 2014 *Nat. Mater.* **13** 1096–1101
[14] Mahjouri-Samani M, Lin M W, Wang K, Lupini A R, Lee J, Basile L, Boulesbaa A, Rouleau C M, Puretzky A A, Ivanov I N, Xiao K, Yoon M and Geohegan D B 2015 *Nat. Commun.* **6** 7749
[15] Hamidani A, Bennecer B and Zanat K 2010 *J. Phys. Chem. Solids* **71** 42–46
[16] Liu X, Zhou H, Yang B, Qu Y and Zhao M 2017 *Sci. Rep.* **7** 39995
[17] Sun J, Shi H, Siegrist T and Singh D J 2015 *Appl. Phys. Lett.* **107** 153902

[18] Oyedele A D, Yang S, Liang L, Puretzky A A, Wang K, Zhang J, Yu P, Pudasaini P R, Ghosh A W, Liu Z, Rouleau C M, Sumpter B G, Chisholm M F, Zhou W, Rack P D, Geohegan D B and Xiao K 2017 *J. Am. Chem. Soc.* **139** 14090–14097
[19] Madhu and Singh R 2011 *Int. J. Hydrog. Energy* **36** 10006–10012
[20] Liang J, Yang Y, Zhang J, Wu J, Dong P, Yuan J, Zhang G and Lou J 2015 *Nanoscale* **7**(36) 14813–14816
[21] Lin J, Zuluaga S, Yu P, Liu Z, Pantelides S T and Suenaga K 2017 *Phys. Rev. Lett.* **119**(1) 016101
[22] Kresse G and Hafner J 1993 *Phys. Rev. B* **47**(1) 558–561
[23] Kresse G and Furthmuller J 1996 *Comput. Mater. Sci.* **6** 15–50
[24] Kresse G and Furthmüller J 1996 *Phys. Rev. B* **54** 11169–11186
[25] Kresse G and Joubert D 1999 *Phys. Rev. B* **59** 1758–1775
[26] Grimme S 2006 *J. Comput. Chem.* **27** 1787–1799
[27] Dingle R, Störmer H L, Gossard A C and Wiegmann W 1978 *Appl. Phys. Lett.* **33** 665
[28] Nguyen L D, Larson L E and Mishra U K 1992 *Proc. IEEE* **80** 494–518